Mobility Enhancement in Amorphous Polyamide 6,6 Induced by Water Sorption: A Molecular Dynamics Simulation Study

Sylvain Goudeau,*,† Magali Charlot,‡ and Florian Müller-Plathe†

International University Bremen, CampusRing 6, 28759 Bremen, Germany, and Rhodia Recherches, 85 rue des Frères Perret, 69192 Saint-Fons Cedex, France

Received: August 6, 2004; In Final Form: September 14, 2004

The local dynamics of water and its effect on the segmental mobility in the amorphous phase of polyamide 6,6 have been investigated. At 300 K and below, where the polymer segments undergo no significant motion (displacements below 2 Å, no reorientation) in the time scale of the simulation, water molecules exhibit mostly orientational freedom, and a bimodal distribution of reorientation times is observed. As the temperature is increased, an increasing fraction of the water molecules also experience hopping behavior between polyamide 6,6 cavities, but true diffusion on a nanosecond time scale is observed only above 400 K. The analysis of amide and methylene group reorientation clearly shows lubrication of the intermolecular amide−amide hydrogen bond, detected above 350 K only at the time scale of 2 ns. This phenomenon goes beyond a simple free volume effect, as is shown through the analysis of the local hydration of individual amide groups. The motion of inner methylene segments is also affected by water, but in a more limited extent. The enhancement of their mobility with water content is probably an indirect effect of the lower reorientation times of neighboring amide groups.

I. Introduction

There has been a growing interest in the past decade concerning inorganic particle filled nylon composites.[1] They can provide, at lower manufacturing costs, increased dimensional stability. The improvement of their mechanical properties (and especially impact strength) is the object of ongoing research, requiring a better understanding of parameters affecting the deformation modes at the micrometer scale, such as filler dispersion and interfacial phenomena occurring at the filler−matrix interface. The influence of water on these deformation modes is critical and arises from much lower length scales, which have been accessed by experimental techniques recently. NMR,[2,3] mechanical,[4−6] and dielectric measurements[4,5,7−12] have been the main tools for investigating the effect of water on the segmental mobility of the amorphous polyamide phase. The interplay of water induced plasticization and hydrogen bonding[13] and the topological constraints due to the neighboring crystalline moieties[14] give rise to a complex spectrum of local relaxation processes. In parallel, a number of molecular dynamics simulation tools have been implemented which allow the analysis of such segmental processes,[15,16] and sometimes a direct comparison with the experimental NMR and dielectric spectra[17,18] through chemically realistic models of polymer chains. This has been carried out only for dry, unplasticized polymers, although the influence of excess free volume has been partly addressed with simulations of poly(ethylene oxide) under negative pressure[19] (recently, corresponding experiments on poly(vinyl acetate)[20] have become available). Some simulations have also investigated the local dynamics behavior in dilute or concentrated polymer aqueous solutions, but the influence of various amounts of water on polyamide local mobility has never been studied so far. It is clearly the goal of the present contribution.

In previous work,[21] the static properties of dry and water-containing polyamide 6,6 have been investigated, displaying a clearly non-homogeneous water organization. On the basis of static, geometric considerations, the water molecules could be sorted between bound and free molecules, according to their location relative to the amide−amide hydrogen-bond network. The influence of this distribution on the unoccupied volume displayed a typical hole-filling behavior at low temperatures and water contents (due to the increased fraction of water molecules bound to or bridging amide groups) and a strong increase of free volume at high temperatures. Intuitively, we would expect a drop of the polymer mobility in the first case and a strong enhancement in the latter. However, as stated above, the experimental mechanical or dielectric relaxation spectra are more complex. The strong decrease in the dynamical glass transition temperature observed even at very low water contents, that is, in the hole-filling regime,[13] is one illustration. This long time scale behavior involving the interplay between water mobility and the polymer main relaxation, α, is extremely difficult to catch in simulations. Indeed, if we consider the experimental Williams−Landel−Ferry (WLF) time/temperature dependence of the α-process,[4] it would be shifted from 340 K at the second time scale to around 470 K at the nanosecond time scale for the dry polymer. As a consequence, we will focus here on local and short-time dynamics only, trying first to investigate if the geometrically (static picture) defined concept of "tightly" or loosely bound water molecules is evidenced dynamically, under various temperature conditions. The resulting influence of water on polyamide (PA) segmental dynamics is then investigated.

* To whom correspondence should be addressed. Phone: 0049 (0)421 200 3560. E-mail: s.goudeau@iu-bremen.de.
† International University Bremen.
‡ Rhodia Recherches.

10.1021/jp046461e CCC: $27.50 © 2004 American Chemical Society
Published on Web 11/10/2004

TABLE 1: Composition of the Simulation Cells at Different Water Contents[a]

system	N_w	N_w/N_{am}	M_w/M_{tot} (%)
PA0	0	0	0
PA2	152	0.16	2.5
PA5	304	0.32	4.8
PA10	608	0.63	9.1

[a] N_w is the number of water molecules, M_w is their weight, and N_{am} is the number of amide groups.

II. Models and Simulation Methods

The polyamide model and simulation protocols are briefly reviewed here. Full details and force field parameters are available elsewhere.[21] Twenty-four independently generated polyamide chains each containing 40 amide groups are simulated at constant pressure (1 bar) and various temperatures for 2 ns. The periodic simulation boxes ($\sim$55 Å)^3 also contain 0, 2, 5, or 10% water, as summarized in Table 1.

Chain Generation. A set of noninteracting chains has been generated by a pivot Monte Carlo (PMC) method,[22] as implemented in the gmq software package.[23] In the PMC simulations, the Monte Carlo moves are the change of randomly picked dihedral angles, to a random value. This method has been proven to generate successfully meltlike conformations of the chains for a broad range of apolar and polar polymers, showing a good agreement with experimental mean radii of gyration, R_g, and end-to-end distances, $\langle r \rangle$.[24−28] It generates ensembles for a phantom chain, in which every atom interacts with neighboring atoms only if they are within a certain interaction range along the chain. With this range correctly chosen, the ensemble corresponds to chains in a θ-solvent or melt. A value of four backbone bonds has been chosen for PA, implying that two neighboring amide groups do not interact with each other.[29] By doing so, we avoid the formation of exclusively intramolecular hydrogen bonds between neighboring amides in the absence of compensating intermolecular ones. This leads to a slight overestimation of $\langle r \rangle$ (7.5 nm, averaged over 1000 configurations) compared to the experimentally available values of dimensions in θ-solvent,[30] computed as 6.1 $\pm$ 0.6 nm for 4500 g/mol chains. Employing a nonbonded interaction cutoff of nine backbone bonds (so that neighboring amide groups fully interact) results in a strongly underestimated $\langle r \rangle$ value, 3.7 nm. The starting configurations for further molecular dynamics simulations are evenly picked from a trajectory of 2×10^6 attempted PMC moves at 300 K, with an acceptance ratio of around 10%.

After this generation stage, the chains are submitted to periodic boundary conditions (PBC), with the full range of intra- and intermolecular nonbonded interactions taken into account, using classical atomistic molecular dynamics (MD).

Molecular Dynamics. The preparation stage, necessary to introduce the intermolecular interactions representative of the polyamide melt, starting from a set of initially noninteracting chains, is composed of three steps:

(1) First, the box size is set arbitrarily to a rather high value, so that the density of the initial cell is around 0.85 g/cm^3 (the experimental value at room temperature is 1.07−1.1).

(2) Then, overlaps between initially noninteracting chains are removed at constant volume (around 10 MD stages of 2000 time steps each, during which the nonbonded ϵ parameters[21] are turned on progressively from 0 to their full value, and the time step is increased from 10^{-6} to 2 fs with a temperature coupling time equal to 10 time steps).

(3) The final stage is carried out in the constant pressure and temperature (NPT) ensemble for 2 ns at 500 K. The length of the time step is 2 fs. Temperature and isotropic pressure (1 atm) are regulated according to Berendsen's method,[31] with coupling times of 0.2 and 5 ps (compressibility 10^{-6} kPa^{-1}), respectively. The chains do not have time to fold before the density reaches the equilibrated value of 0.99−1.03 g/cm^3, depending on water content. The introduction of water molecules, as described and justified in a further section, takes place at the beginning of this NPT stage at 500 K.

The cells are then submitted to a continuous cooling at constant pressure, with a 0.25 K/ps cooling rate. The configurations extracted at the desired temperature from this cooling-down stage constitute starting points for further NPT production simulations during which the properties of interest are analyzed. The length of the time step is 2 fs. The Berendsen thermostat and manostat are used with coupling times of 0.2 and 5 ps (isothermal compressibility 10^{-6} kPa^{-1}), respectively. A Verlet neighbor list with a pair cutoff of 1.0 nm is used and updated by a link-cell scheme every 30 steps. Bond constraints are maintained to a relative tolerance of 10^{-6} by the SHAKE procedure.[32] The functional form of the force field employed and more details concerning the MD simulation program YASP can be found elsewhere.[33]

Water Inclusion. Water is described by the SPC/E model.[34] The simulations of water-swollen polymers use in their vast majority[35−37] simple combination rules to include SPC water in their force field description of hydrogen-bonded, hydrated systems.

The interactions between various water models and amide groups have been extensively studied in simulations of biological molecules[38−40] and compared with ab initio data. The OPLS-AA force field succeeded in reproducing the free energy of hydration of several methyl-substituted amides and amines[38,39] in contact with SPC or TIP4P water, without the requirement of additional polarization terms in the initial force fields. All condensed-phase energetic properties are perfectly reproduced.

The water molecules are added at the beginning of the first NPT stage at 500 K, as stated before. Molecules are inserted in a totally random way, regarding their position and orientation. In the literature, the simulations of water-containing polymer systems are often carried out at constant temperature, and water is introduced at bulk density at the beginning of the simulation. This allows the formation of two-to-three-membered small clusters, starting from random water positions, but the formation of larger-scale patterns is prevented at high polymer concentrations by the low diffusion coefficients of water at room temperature. Introducing water at 500 K, in our case, enables every molecule to travel the whole box size (5 nm) during the first nanosecond of equilibration. Visual observation and cluster analysis of simulations at 500 K show no phase separation; the available literature data (experiments and semiempirical Flory−Huggins fit) for PA6,6 melts[41,42] at such temperatures suggest a solubility of at least 11% water. The PA−water interaction parameter, χ, is increasing with temperature above 500 K,[42] so the solubility should be higher at lower temperatures.

The initial configurations of these NPT runs are evenly grabbed from the cooling-down trajectory, every 25 K between 500 and 100 K and pre-equilibrated for 500 ps. The duration of the production simulations is 2 ns; snapshot conformations are extracted and recorded every 0.8 ps. Two configurations have been studied for each water content. One has a root-mean-square (rms) radius of gyration, R_g, of 24.5 Å and a mean-squared end-to-end distance of 59 Å, and the other has R_g =

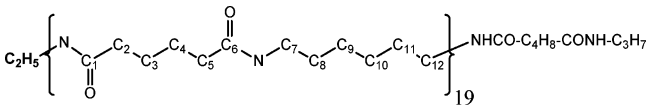

Figure 1. Structure of the polyamide chains simulated in this work, with carbon labeling.

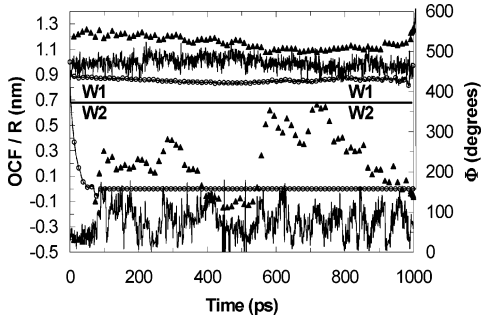

Figure 2. Displacement, *R* (triangles), orientation, Φ, of the dipole moment vector (lines), and the corresponding autocorrelation function (dotted lines) of W1 and W2. The displacements are reported as the norm of the position vector of the oxygen atoms, where the origin is defined as the initial position of the water molecule. The corresponding curves have been conveniently shifted along the vertical axis for clarity. The orientation of the dipole moment vector is its angle with the *x* axis.

27.5 Å and $r = 75$ Å, respectively. The structure of the chains is displayed in Figure 1 with carbon labeling for further reference.

III. Results and Discussion

3.A. Water Dynamics. Depending on their local environment (other water molecules, amide groups, and methylene moieties), water molecules in polymers can be found in different mobility states.[35,37] The time development of the orientation and position of two single water molecules displayed in Figure 2 (PA10 at 300 K) illustrates two different types of dynamical behavior. The first water molecule (W1) is, according to our hydrogen-bond criterium,[43] bonded to two neighboring amide groups for 60% of the simulation time and could be defined as a bridging molecule. The second one (W2) occasionally shares hydrogen bonds with other water molecules but never directly with any amide group. While W2 moves to different sites in the polymer matrix (displacements of more than 1 nm in 1 ns, whereas no polymer atom travels more than 3−4 Å), the translation of W1 is limited to 2 Å which corresponds to the amplitude of motion of the local polymer site. The different behaviors of W1 and W2 are also evidenced by the angular motion of their dipole moment vectors which display a background of low-amplitude librations interrupted by "jumps" of up to 30° for W1 and more than 120° for W2. The average amplitude of angular moves is much more important for W2, as well as the jump frequency. In the case of W1, the longer time scale angular drifts (30° in 400 ps) are probably related to the orientation of neighboring polyamide chains (backbone or carbonyl/amine bond vectors) delimiting its local "cage", which display similar time development (not shown in Figure 2). W1 and W2 are arbitrarily referred to as "immobile" and "mobile" water molecules, respectively. This subdivision between mobile and immobile molecules is of course time scale dependent: W2 can be considered as mobile only as long as it does not reach any available amide site (that is both accessible and not already bonded with water), which is the case here at the 2 ns time scale and 300 K. Moreover, it is a bit oversimplified: some molecules display the translational behavior of W1, whereas they are not bonded to any amide according to the hydrogen-bond criterium but are caged in small cavities in methylene moieties. Their angular motion is in most cases an intermediate between the W1 and W2 behaviors. As a consequence, the orientation autocorrelation functions of the dipole moment vector of each water molecule, W*i*(OACF$_i$), also displayed in Figure 1 for W1 and W2, exhibit a broad range of relaxation times. The analysis of the correlation between the reorientation dynamics of a single water molecule and the history of its hydrogen bonding to polymer or other solvent molecules has already been carried out,[44] so this kind of analysis will not be detailed further here. Rather, we focus on the overall distribution of individual water molecule behaviors regardless of their very local/temporary environment.

Water Reorientation. Let's first investigate the distribution of reorientation dynamics among water molecules in the system. We would like to check if the different behaviors of W1 and W2 are representative of two or more well separated classes of water molecules or if they are part of a continuous, broad distribution of individual molecule dynamics. In this purpose, the OACF$_i$ and their resulting average over all water molecules, D-OACF, have been computed as

$$\langle \cos \theta \rangle_{(t)} = \langle \mathbf{u}(t_0) \cdot \mathbf{u}(t + t_0) \rangle \qquad (1)$$

where **u** is the normalized dipole moment vector and the average is over all time origins (OACF$_i$) and all water molecules (D-OACF). Let's first discuss the individual components of the OACF.

The OACF$_i$ of an individual water molecule, W*i*, obeys a single exponential time decay, with a temperature-dependent prefactor, $A \sim 0.9$:

$$\mathrm{OACF}_{i(t)} = Ae^{-t/\tau_{\mathrm{W}i}} \qquad (2)$$

For the two example molecules, W1 and W2, the relaxation times are $\tau_{W2} = 16.5$ ps and $\tau_{W1} = 4500$ ps. The distribution of τ_{Wi} as a function of temperature for PA10 is displayed in Figure 3. We observe a qualitative change between 300 and 350 K.

At low temperatures (300 K and below), the relaxation time distributions are clearly bimodal. The histograms fit with two log-normal distributions, centered around $\tau_1 = 100$ ps and $\tau_2 = 5$ ns, respectively. The main influence of temperature, in this range, is to increase the amplitude of the τ_1 mode with respect to the amplitude of τ_2. One would also expect a shift of τ_1 and τ_2 to lower values, as well as a broadening of the corresponding distributions.[44] These two effects are rather limited below 300 K.

Above 300 K, the fast mode survives, τ_1 shifts to shorter times (∼20 ps at 500 K), and the distribution becomes narrower. It is not clear if there is a separate long-time relaxation mode or if the single mode distribution merely has a long tail. One can notice the relatively high value of τ_1 (∼100 ps at 300 K, 30 ps above 400 K), related to the most mobile molecules in the system and yet much larger than the relaxation time ($\tau \sim$ 10 ps at 300 K) of the dipole moment correlation function of water molecules in bulk water or dilute polymer solutions.[44]

We have attempted (Figure 3E) to resolve separately the contributions of molecules differently hydrogen bonded to the polymer matrix to the overall bimodal distribution of relaxation times at 250 K. For each water molecule in the PA10 system, the average number of hydrogen bonds, $\langle N_{\mathrm{hb}} \rangle$, shared with the polymer amide groups has been computed according to the aforementioned hydrogen-bond criterion during the 2 ns simula-

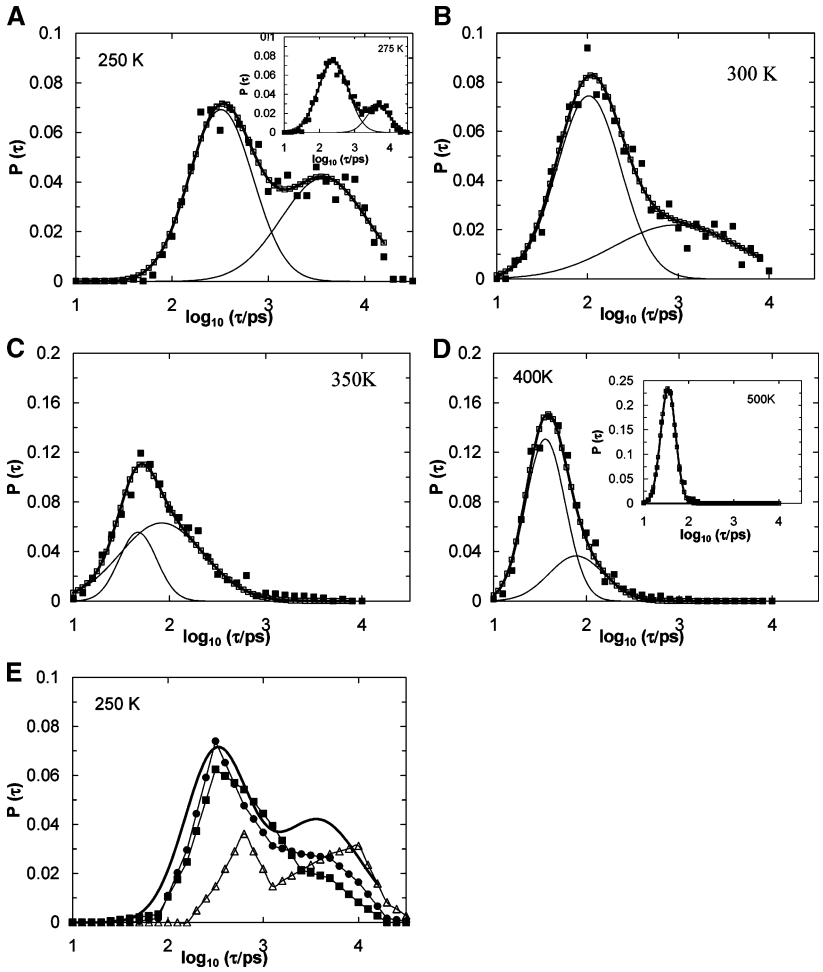

Figure 3. Distribution of $OACF_i$ relaxation times as a function of temperature for PA10. (A−D) Symbols, raw data; line going through the symbols, fit to the data (sum of two normal distributions); thin curves, individual normal distributions. All probabilities are normalized to integrate to 1. (E) Details of the distribution of relaxation times at 250 K. Bold line: overall distribution. Lines going through the symbols: $\langle N_{hb}\rangle < 0.05$ (squares), $\langle N_{hb}\rangle = 1.0 \pm 0.2$ (circles), and $\langle N_{hb}\rangle = 2.0 \pm 0.2$ (triangles).

tion. The overall correlation coefficient between $\langle N_{hb}\rangle$ and τ_{Wi} is close to 0.4. As expected, the rotational motion of water molecules sharing more hydrogen bonds with the polymer is slower. Three subsets of about 100 water molecules have been considered, with $\langle N_{hb}\rangle < 0.05$, $\langle N_{hb}\rangle = 1.0 \pm 0.2$, and $\langle N_{hb}\rangle = 2.0 \pm 0.2$, respectively. The relaxation time distributions corresponding to the three subsets all exhibit both τ_1 and τ_2 components, but it should be noticed that a significant qualitative change occurs between $\langle N_{hb}\rangle = 1.0$ and $\langle N_{hb}\rangle = 2.0 \pm 0.2$, with a dramatic increase of the population of the τ_2 mode, whereas little difference is observed between $\langle N_{hb}\rangle = 0$ and $\langle N_{hb}\rangle = 1$. It means that a great part of the τ_2 mode is related to bridging water molecules, tightly bound to different amide groups of the polymer matrix.

Overall Relaxation Behavior−Water Concentration Dependence. The overall D-OACF are represented at selected temperatures in Figure 4.

The corresponding curves cannot be fitted to a single Kohlrausch−Williams−Watts (KWW) equation, due to the uneven distribution of individual orientation correlation times outlined previously. The best fit to the D-OACF is obtained using a modified KWW equation:

$$\langle \cos\theta\rangle_{(t)} = A_1 e^{(-(t/\tau_1)^{\beta})} + A_2 e^{(-(t/\tau_2)^{\beta})} \qquad (3)$$

with $A_1 + A_2 < 1$ to disregard the fast decorrelation below 2 ps which is not related to the processes of interest. The correlation

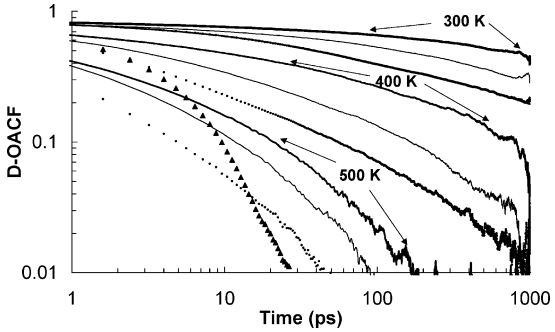

Figure 4. Autocorrelation function of the dipole moment vector of water molecules (averaged over all molecules in the system) at 300, 400, and 500 K. Thick curves, PA2; thin curves, PA5; dots, PA10. The D-OACF of bulk water (2700 SPC/E molecules in the NPT ensemble at 300 K) is also displayed for comparison (triangles).

times t_1 and t_2 are computed as the time integral of the corresponding exponentials:

$$t_{1,2} = \int_0^{\infty} \exp\left(-\left(\frac{t}{\alpha}\right)^{\beta}\right) dt = \frac{\alpha}{\beta}\Gamma\left(\frac{1}{\beta}\right) \qquad (4)$$

The evolution of D-OACF can be explored this way only above 250 K; the decorrelation is too low below this temperature. As expected at intermediate temperatures, the average D-OACF displays faster reorientation of water molecules when their concentration is increased from 2.5 to 10 wt % in PA, whatever

TABLE 2: Fitting Parameters of eq 3

T (K)	system	$A1$	$\Phi = A1/(A2 + A1)$	t_1 (ps)	t_2 (ps)	β_1	β_2
300	PA10	0.15	16	36	1200	0.87	0.3
325	PA10	0.10	10	15	200	0.99	0.27
350	PA10	0.50	47	9	250	0.41	0.28
375	PA10	0.53	59	6	210	0.568	0.40
400	PA10	1.26	86	2	160	0.32	0.41
500	PA10	0.73	87	1	20	0.50	0.59
300	PA2	0	0		13000		0.35
325	PA2	0.08	9	70	12000	1	0.24
350	PA2	0	0		1500		0.35
375	PA2	0.04	4	23	450	1	0.22
400	PA2	0.03	3	2	170	1	0.34
450	PA2	0.14	22	3	70	1	0.47
500	PA2	1.26	100	3		0.27	

the temperature. Even at the lowest temperature studied here (200 K, not shown), this mobility enhancement upon increasing concentration is noticed, whereas we could have expected a small decrease at high water concentrations, if the free volume around the water molecules was not even enough to allow their rotation. In Table 2 are listed some values of the fitting parameters of eq 3 and the relaxation times t_1 and t_2 for PA10 and PA2.

The correlation time t_1 for pure water at 300 K is around 5 ps; t_1 varies from 35 to ~100 ps at this temperature for water in PA. t_2 is typically around 2 orders of magnitude bigger. This distribution of t_1 and t_2 agrees rather well with the τ estimates obtained from the individual OCF of each water molecule. W2 has, for example, $\tau = 16.5$ ps, and W1 has $\tau > 1$ ns. If t_1 is related to the decorrelation time of a water molecule "unbound" to PA, it would not be expected to vary significantly with water contents. It appears, though, that t_1 depends as much as t_2 on the water contents in PA. The ratio of $A1/(A1 + A2)$ can be qualitatively related to the amount of "free" molecules in the system, which is as expected greater for PA10 than PA2 and increases with temperature. t_2 at 500 K has the same order of magnitude as the relaxation time of the amide reorientation OCF (see Figure 12), whereas it is significantly lower at intermediate temperatures. Rather than a measurement of the "bound water"/amide correlated orientation, t_2 is a consequence of the hydrogen-bond lifetime at these temperatures. Subsequently, the terms of tightly or loosely bound molecules are meaningful only at low temperatures and time scales not much greater than t_2, that is, some nanoseconds at 300 K.

Water Hopping. A good picture of water dynamics can also be obtained by counting the number of site−site jumps accomplished by a water oxygen during the course of the simulations, as seen in Figure 2 in the case of W2 (mobile molecule). We define a jump as a displacement greater than a threshold value and achieved within 30 ps. The positions of water molecules are preaveraged over 10 ps (12 successive configurations). The amplitude threshold is aimed at excluding ballistic motions of water molecules bouncing inside the largest PA cavities ("void" spaces between polymer chains). Their average radius at 300 K is reported not to exceed 3−3.5 Å.[13] Several threshold values have been tested, ranging from 5 to 9Å. We have found that results converge for jump amplitudes greater than 7 Å, so the discussion is restricted to this value.

According to this criterion, W2 undergoes three jumps (at 80, 570, and 730 ps) during the 1 ns fraction of the trajectory reported in Figure 2. The jump frequency per molecule, as shown in Figure 5, varies as a function of water contents and temperature between 2×10^6 (the detection limit) and 3×10^{10} s^{-1}.

The jump frequency above $\log(f) \sim 9.5$ in Figure 5 is affected by saturation effects (the jump frequency is limited by the configuration sampling—0.8 ps—and averaging—10 ps—time intervals); defining the dynamics of water in terms of jumps is less sensible when the temperature is raised to 500 K, where the displacement of water molecules becomes more continuous and does not exhibit immobile stages between consecutive hops. In the low temperature range, the jump frequency displays an Arrhenius temperature dependence, with an average activation energy depending on the jump amplitude criterion (5−9 Å).

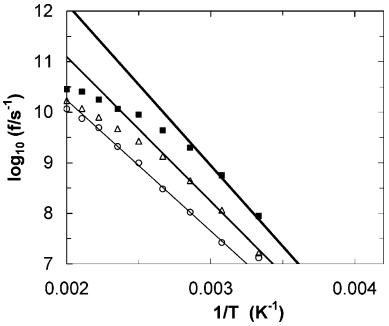

Figure 5. Jump frequency per molecule as a function of temperature and water contents, with an amplitude threshold of 7 Å: circles, PA2; triangles, PA5; squares, PA10. The solid lines are linear fits to the data at low temperatures.

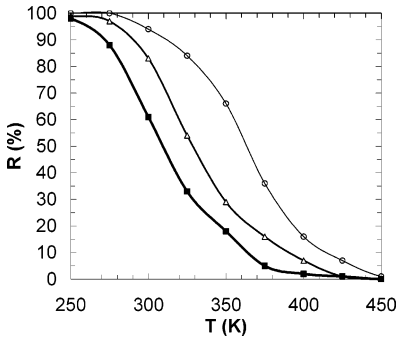

Figure 6. Percentage of immobile molecules (undergoing no jumps in 1 ns) as a function of temperature and water contents: circles, PA2; triangles, PA5; squares, PA10.

The activation energy, E_a, obtained from the slope of the Arrhenius plots below 375 K remains remarkably constant for threshold values above 7 Å (56 kJ/mol) and drops off below 6 Å (43 kJ/mol with a 5 Å threshold). The value of 56 kJ/mol, averaged over all water contents, corresponds to the experimental activation energy of water diffusion in PA, given[30] as 58 kJ/mol. Thus, we consider that such jumps are the dominant process in water diffusion at low temperatures (<400 K). The water concentration dependence of E_a is not accurate. Values spread from 52 ± 5 kJ/mol for PA2 to 62 ± 5 kJ/mol for PA10. The experimental diffusion coefficients are measured at water saturation (~12−15 wt % in PA), so they would correspond better to the latter value.

The fact that the activation energy is found constant only above the 7 Å cutoff reveals that short-time (nondiffusive) processes such as intracluster or intracavity motion can reach this length scale, which is finally not surprising: the average hole radius of 3 Å only does not take into account the size dispersion or shape distribution of the cavities.

The percentage of water molecules undergoing no jumps in 1 ns, arbitrarily referred to as immobile molecules further in the text, is represented in Figure 6 which is a perfect illustration of a two-step sorption model[5] between 300 and 350 K. According to this mechanism, sorption of water up to 3% in the amorphous phase would result mainly in "tight" amide−water−amide hydrogen bonding; additional sorbed molecules,

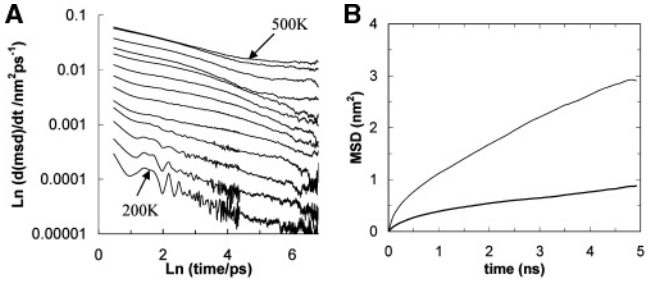

Figure 7. (A) Time derivative of the MSD as a function of time, for PA10, from 200 to 500 K at 25 K intervals. (B) MSD as a function of time, for PA10. Thin line, 350 K; bold line, 300 K.

termed as loosely bound, cluster between the first molecules and remaining available amide sites. At 350 K, the percentage of immobile molecules drops from approximately 60% for PA2 to 30% for PA5 and 15% for PA10. This means that nearly every additional molecule beyond the concentration of 2.5% is a mobile one. Let's assume that PA5 is obtained by adding N1 water molecules to PA2, and PA10 by adding N2 = 2N1 water molecules to PA5. At 300 K, whereas 5% only of the water molecules of the PA2 system are mobile, 30% of the N1 molecules are mobile and 60% of the remaining N2 ones are mobile. Obviously, the values presented here are arbitrary, but Figure 6 clearly points out that water molecules are not all dynamically equivalent at the nanosecond time scale.

The proportion of mobile and immobile molecules displayed in Figure 6 shows the same temperature trend as the proportion of "fast" and "slowly" rotating molecules corresponding respectively to the short-time log-normal distribution, t_1, and the long-time or tail distribution of $OACF_i$ relaxation times: a large majority of water molecules is mobile (in translation or rotation) above 350−375 K for PA10. There is however a distinction at 300 K, where most molecules are immobile in the polymer matrix, but half of them still display fast reorientation dynamics according to Figure 3.

Water Diffusion. A common way to investigate the mobility of a solvent in polymers is to analyze the time development of the mean-square displacement (MSD) defined as

$$\mathrm{MSD} = \langle(\mathbf{r}(t) - \mathbf{r}(t_0))^2\rangle \tag{5}$$

where **r** is the position vector of a water oxygen and the average is performed over all time origins, t_0.

The time derivative of the MSD at various temperatures for PA10 is represented in Figure 7A. Einstein diffusive behavior should manifest itself as a plateau value of the derivatives at long time scales. This diffusive regime is found only above 425 K. A limited set of simulations undertaken for longer times (up to 10 ns, for PA10 at 300, 350, and 400 K) did not allow observation of Einstein behavior below 400 K, despite of the displacements of up to 2 nm that are achieved by water molecules (350 K). Anomalous diffusion of water in hydrogen-bonding polymers has often been reported.[36,45] Figure 7B shows that the diffusive process is only "guessed" after 2 ns at 300 K, and only an upper limit of the diffusion coefficient at this temperature can be estimated (0.5×10^{-8} cm^2/s). However, to have a global overview of the mobility of water molecules at different concentrations and temperatures, we have plotted in Figure 8 an "apparent" diffusion coefficient

$$D = \lim_{t\to\infty} \frac{1}{6} \frac{\mathrm{d(MSD)}}{\mathrm{d}t} \tag{6}$$

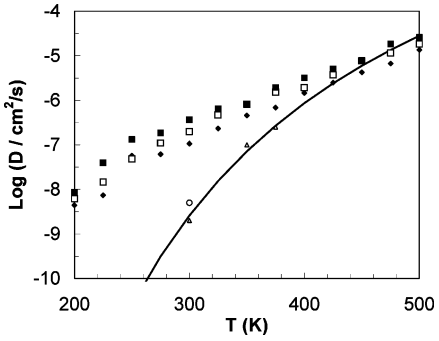

Figure 8. Apparent diffusion coefficients as a function of temperature. Triangles and solid line: experimental data[15] and fit with a 58 kJ/mol activation energy. Symbols, simulation data: filled squares, PA10; open squares, PA5; filled diamonds, PA2. Open circle: *D* from MSD of Figure 7b (extended run of 5 ns instead of 2 ns).

computed by fitting a straight line to the MSD between t = 500 ps and t = 1.8 ns.

At all temperatures, the diffusion coefficient increases with water contents. The dependence, however, is small above 400 K where short-length-scale motions do not contribute to the apparent diffusion coefficient, much below a factor of 10 between PA2 and PA10.

3.B. Water Influence on Polyamide Dynamics. A key parameter, which allows for the investigation of the dynamics of amide−amide or amide−water interactions is the amide carbonyl and amine orientational autocorrelation function (CONH-OACF). It is defined as in eq 1, but the reorienting vector is the CO or NH bond vector, respectively. The correlation functions of CO and NH orientations are very similar, so only their average is discussed. The reorientation of amide groups, resulting in intermolecular hydrogen-bond creation or breaking,[2] is usually associated in the literature to the γ-process observed in dielectric spectra.[11,12] The OACF of methylene C−H vectors has also been computed, to investigate the contribution (if any) of the methylene moieties to the overall enhancement of PA segmental dynamics upon water sorption. We proceed in this section similarly to the discussion of water reorientation (section 3.A): We compute first the correlation functions ($OACF_i$) of individual bond vector orientations (carbonyl or amine, or methylene C−H). This allows us to obtain a distribution of different behaviors as a function of the local environment of amide groups. Then, the overall OACF, averaged over all bond vectors in the system, is analyzed to assess the water influence at a larger scale, to compare it with experimental observables.

Local Environment Analysis. The local water or carbon environment of carbonyl, amine, and inner methyl groups of the hexamethylene moieties (C_9−H and C_{10}−H) is defined as the average number of species (water oxygen and methylene carbon) found in a sphere with a radius of 0.38 nm centered on the relevant carbon or nitrogen atom, during 1 ns of simulation. The same duration is used to compute the $OACF_i$. The $OACF_i$ are too noisy to be fitted to a single (extended) exponential decay. Therefore, we use arbitrarily their value at 500 ps as a measurement of the amount of decorrelation achieved in a given environment. Using another value (for example, 100 ps) did not change the qualitative trends discussed in this section. The radius of the "environment sphere" was chosen small enough to resolve separately the different environments of adjacent amide and methylene moieties. It also provides the side result that half of the C−O/N−H groups at 300 K have no water in their close environment, which is consistent with indirect experimental data. The $OACF_i$(500 ps), averaged over bins

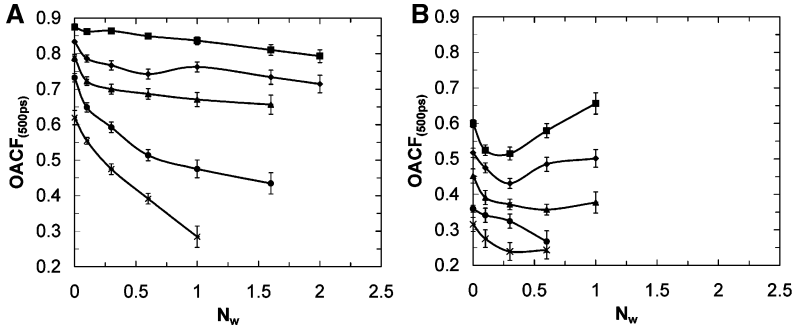

Figure 9. Orientational correlation functions (value at 500 ps) of CO/NH bond vectors (A) and $C_9-H/C_{10}-H$ (B) as a function of the local water density, N_w: squares, 300 K; diamonds, 325 K; triangles, 350 K; circles, 375 K; crosses, 400 K.

corresponding to different numbers of water molecules, N_w, in the sphere, are displayed in Figure 9 versus N_w and temperatures between 300 and 400 K. Above 400 K, water is so mobile that almost all amide/methylene groups have on average the same water environment.

At 300, 325, and 350 K, all plots (Figure 9A) display the same trend: A strong and statistically significant decrease of the average OACF is observed between 0 and 0.1 water molecules only. When the local concentration of water is increased from 0.1 to 1.5 or more, the additional decrease, if any, is much slower. This trend cannot be correlated with the experimental concepts of water plasticization. It is more likely to be a simple free volume effect: The local carbon density, N_c (not shown), drops by 10% when the local water density is increased from $N_w = 0$ to $N_w = 0.1$ and remains constant at higher water contents. In other words, the amide groups which are buried in regions of high PA density reorient more slowly than those which are located in lower density areas. Water molecules can access the latter ones and not the former ones but have by themselves no effect on amide dynamics at these low time scales.

At 375 K and above, one can notice a decrease of OACF over the whole water density range. Replacing amide−amide interactions by water−amide ones results in a mobility enhancement, independent from free volume considerations. N_c does not decrease for $N_w > 0.1$ or 0.3, which means that the unoccupied volume in the amide-centered sphere does not increase when more water is added. It would be tempting to correlate the shape of the plot at 375 K (strong decrease up to 0.6 water/amide, slower decrease for higher water amounts) with the experimental T_α versus water content curves. T_α, the water plasticized main relaxation temperature measured in dynamical mechanical or dielectric experiments, also displays a strong initial drop up to 3−4% water (in the amorphous phase) followed by a slower decrease upon further water addition. This is often interpreted in conjunction with a dual sorption model speculating that most of the amide bonds initially available to water have already been "bridged" by water molecules up to 3−4%, with further addition of water leading to few additionally bridged amide−amide bonds. We observe exactly the same trend here, and taking into account the fact that half of the amide groups are not accessed by water, the value of 0.6 water molecules per amide (corresponding locally to 8 wt % water) at the slope change very well matches the experimental one.

Considering the temperature dependence of the OACF at a given water density, note also that the "transition" in the OACF behavior between 350 and 375 K mainly affects the amide groups which have on average one or more water molecules in their close neighborhood. This represents only a small fraction (10% or less) of all amide groups in the system and brings only a small contribution to the overall OACF discussed in the next

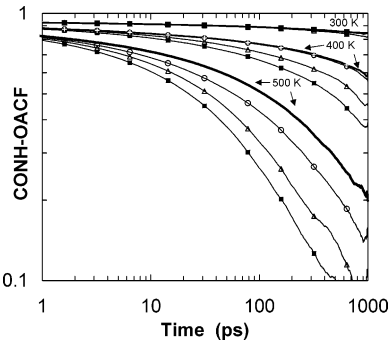

Figure 10. Orientation autocorrelation function for amide groups (C−O and N−H bond vectors) at selected temperatures. Bold lines: PA0. Lines going through the symbols: circles, PA2; triangles, PA5; squares, PA10.

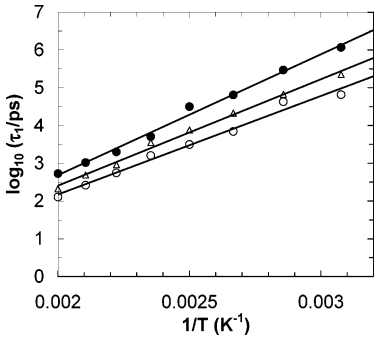

Figure 11. Arrhenius plot of the relaxation time of CONH-OCF for different water contents: filled circles, PA0; triangles, PA5; open circles, PA10.

section, whose relaxation times display Arrhenius behavior over the 300−500 K temperature range. Moreover, we have focused here only in a narrow time scale window, and the OACF temperature dependence at different time scales (or the OACF overall relaxation times, see Figure 11) need not follow the previous trend. Figure 9 gives however a satisfactory qualitative picture of the local mechanisms inducing enhanced plasticization in water-loaded polyamide.

Concerning the inner methylene moieties, similar trends are observed: a strong initial short-time mobility enhancement up to $N_w = 0.1$ water/amide, followed by an ongoing decrease upon further water addition only above 350 K (note however the bad statistics above 0.3 amide/water). Below 350 K, one may even notice slowing down of the $C_{9,10}-H$ reorientation dynamics above 0.3 water/amide at the 500 ps time scale. This may have to do with the additional steric hindrances introduced by caged water molecules; we have shown in a previous section that 60% of them can be considered as immobile at 300 K for PA10. It is also consistent with positron annihilation spectroscopy (PALS) analysis,[13] which shows a so-called antiplasticization effect of

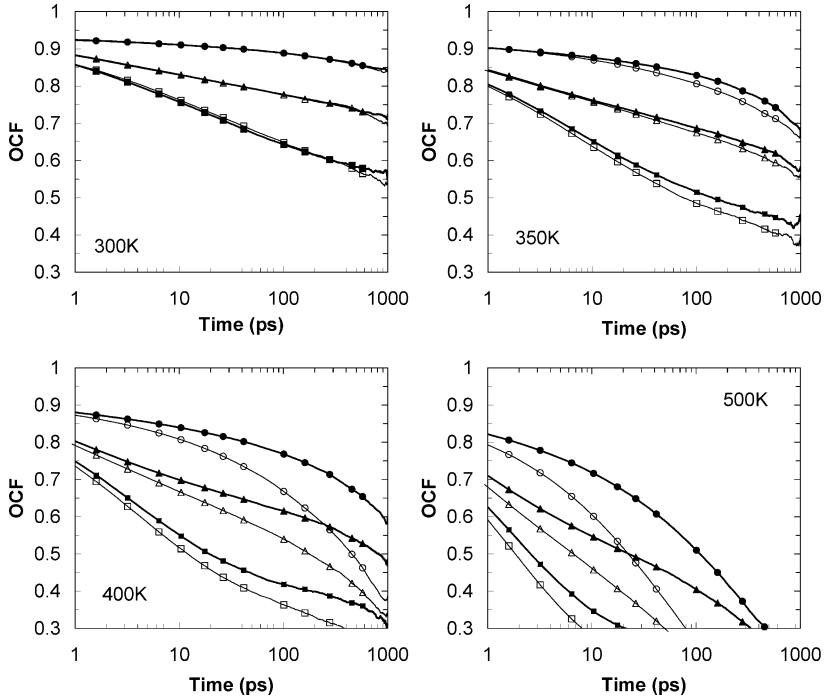

Figure 12. Orientation correlation functions of CO−NH and normalized CH bond vectors in the hexamethylene moiety for PA0 (filled symbols) and PA10 (open symbols): filled circles, CO/NH−PA0; open circles, CO/NH−PA10; filled triangles, C_7C_{12}−PA0; open triangles, C_7C_{12}−PA10; filled squares, C_9C_{10}−PA0; open squares, C_9C_{10}−PA10.

water at low temperatures (decrease of the free volume fraction available for polymer motions). At such water contents, antiplasticization is experimentally observed much below room temperature. The low simulation time scales may be the reason this phenomenon is observed here up to 325 K.

Overall Amide and Methylene Dynamics. The short-time development of the overall amide (CO and NH) CONH-OACF is shown in Figure 10 at selected temperatures. At 300 K, the very slow decorrelation of the OACF allows only a small dependence upon water content at this time scale, the slowest reorientations being observed for PA10 and PA0 and the fastest ones for PA5 at time scales greater than 100 ps. The trends displayed at higher temperatures are more familiar, with a strong enhancement of CONH orientational mobility upon water contents. Note however that, up to 400 K, the PA2 amide groups are hardly more mobile than the PA0 ones (still at the nanosecond time scale), due to the low mobility of most of the PA2 water molecules, outlined previously. The orientational mobility enhancement above 350 K is really an effect of water molecules, and not simply a free volume effect, as this was shown in the previous section. The CONH-OACF can be fitted quite well to a single stretched exponential, thus yielding a correlation time, t_1, computed as the time integral of the KWW function. The variations of t_1 with temperature are displayed in Figure 11 for PA0, PA5, and PA10.

To the precision of the results, the variation of t_1 can be fitted to an Arrhenius temperature dependence, over the whole temperature range 325−500 K. The limited decorrelation of CONH-OACF at 300 K and below yielding excessive uncertainty, close to 1 order of magnitude, about the corresponding relaxation times. The apparent activation energy, E_γ, of this process is 61 ± 5 kJ/mol for PA0 and 49 ± 5 kJ/mol for PA10.[46] Dielectric measurements on Nylon12 provided a qualitatively similar E_γ dependence on water concentration for the γ-process, with 28 kJ/mol for dry systems and 24 kJ/mol at saturation.[8] An average E_γ value of 40 ± 2 kJ/mol was initially reported for dry polyamide 6,6,[4] while the moisture dependence of this value had seemingly not been investigated. Some more recent measurements are closer to the previous simulation values,[47] 38 kJ/mol for wet polyamide 6,6 to 46 kJ/mol for the dry one. These results can also be correlated with ^{2}H solid-state NMR analysis of N−D motions,[2] which reveals an activation energy of 34 kJ/mol for the relaxation time of the jump component of N−D motions (Nylon 6,6 with 0 and 2% water).

The motion of methylene moieties is obviously also affected by the presence of water. We have represented in Figure 12 the orientation correlation function of C−H bond vectors, according to the carbon sequential position in the hexamethylene moiety (see Figure 1 for carbon labeling). C_7 and C_{12} represent the carbons closest to the amide group. As their motions are similar by symmetry, the corresponding orientation functions have been merged into single curves denoted C_7C_{12}. The data concerning C_8 and C_{11} have been omitted for clarity: they fall between C_7C_{12} and C_9C_{10}, being closer to the latter. End-group carbons are excluded from the computation. Unlike the CONH-OACF, the OACF of C−H bond vectors cannot be fitted to a single exponential. The quick decorrelation at short time scales and the slowing-down effect of neighboring CONH groups at longer time scales result in a complex relaxation plot.

At all temperatures, the mobility of CH_2 groups depends on their position in the chain. The groups C_7C_{12} next to the amide moieties are the slowest. The methylenes C_9/C_{10} relax fastest. The behavior of the tetramethylene chain (C_2−C_5) is very similar (not shown).

The water content affects the CH_2 relaxation differently at different temperatures: it has almost no effect at 300 K on the C−H or CO−NH dynamics in the 1 ps−1ns time scale. One may even notice, if statistically significant, some slowing down of inner methylene moieties (C_9C_{10} and C_8C_{11}). This is consistent with the data of Figure 9, showing slowing down of C_9−H/C_{10}−H reorientation in the presence of a high fraction of immobile water molecules. At short time scales, the steric hindrances due to water molecules limit the motions of inner methylene moieties which are responsible for the fast decorre-

lation of OCF between 1 and 100−200 ps. At longer time scales, the increased probability of site−site jumps may cancel this short-time effect. Differences between PA0 and PA10 consistently increase with temperature above 350 K. There are various possible explanations. The most likely, however, is that the lubrication of amide−amide contacts by water indirectly results in an acceleration of the CH_2 relaxation. At short time scales, the amides are the slowest relaxing groups and they restrain the motion of methylene moieties connected to them. The role of amides as impediments for CH_2 relaxation is evidenced by the fact that CH_2 groups further away from the amide relax faster. At high temperatures, another effect probably plays a significant role, namely, the additional unoccupied volume caused by the presence of highly mobile water molecules. The positron annihilation spectroscopy (PALS) data published in the literature clearly distinguish two regimes:[13] at low temperatures or water contents, water takes up free volume, reducing the volume of the cavities in the polyamide matrix (hole-filling antiplasticization regime); at high temperatures or water contents, the inverse effect is observed (plasticization regime). The temperature-dependent enhancement of CH_2 mobility can be attributed mainly to the lubrication of amide−amide interactions at low temperatures (see Figure 9, between 350 and 375 K), with an increasing effect of plasticization at higher temperatures.

As a summary, the motion of amide groups is enhanced by the substitution of amide−amide by amide−water interactions, an effect which could be termed as "lubrication". The motion of methylene groups is indirectly enhanced by the lubrication of amide−amide interactions and also affected by antiplasticization at low temperatures and plasticization at higher temperatures.

Conclusion

The aim of the present study has been to elucidate the motion of water molecules solvated in polyamide 6,6 and its repercussions on the polymer dynamics. The emerging picture is consistent but diverse. First, lo and behold the dependence of water mobility on temperature and water concentration behaves as expected. Higher temperatures and higher water contents lead, in general, to faster translation and reorientation of water. There is some evidence for mutual amplification of the two contributions. Going from 2% water to 10% water accelerates most types of motion disproportionately more at 500 K than at 300 K.

Second, at low temperatures, water molecules may fall into at least two dynamical classes. Their population separates into fast moving and slow moving individuals. Evidence for this is the bimodal distribution of water reorientation times at $T \leq 300$ K as well as the presence of diffusing and nondiffusing molecules below 350 K. At higher temperatures, the bimodality disappears and it is no longer possible to discern slow and fast water molecules. This is in agreement with previous simulations on water-swollen poly(vinyl alcohol),[37] which found evidence for two dynamical states of water molecules *exclusively below* 273 K. The temperature where the fast and slow populations merge is higher in the present case (between 300 and 350 K), possibly owing to the lower water content and the stiffer polymer matrix. It is tempting to relate the bimodal water dynamics, where present, to the concept of bound (by amide groups) and unbound water molecules. While we can classify the hydrogen bonds of a water molecule into those to amide and those to other water, we have, however, not found a clear connection between the mobility on a water molecule and its immediate environment.

Third, only at high temperatures is it possible to calculate reliable water diffusion coefficients. At $T < 400$ K, the diffusion is too slow to allow an evaluation of a diffusion coefficient from a simulation of a few nanoseconds. The values reported are only upper limits. The activation energies derived from an Arrhenius analysis are systematically too low. Turning to the elementary diffusion process, namely, jumps of water molecules between different residence sites, the picture changes somewhat. The activation energy for the jump rate is 56 kJ/mol, in good agreement with the experimental activation energy of the diffusion coefficient of 58 kJ/mol. This not only confirms that activated jumps are the primary mechanism for water diffusion, but it also indicates that, even if diffusion coefficients remain out of range for molecular dynamics simulations, their activation energies may be accessible by concentrating the analysis on the dominant elementary process.

Fourth, both temperature and water contents enhance the short-time reorientation of amide groups as well as methylene groups. The water influence on the global reorientation rates is almost negligible at 300 K but gets much stronger at 400 K and above. Methylene groups reorient faster than amide groups. Their mobility is higher if they are farther away from the nearest amide group along the chain. Thus, amide−amide interactions also restrict the motion of the attached methylene groups. If the former are lubricated by water molecules, the motion of methylene groups is affected too but in an indirect way.

Finally, a detailed analysis shows that the reorientation of individual amide groups depends on their local hydration status: The more water molecules there are in the immediate neighborhood, the faster the amide reorients. This is found at all temperatures, but the effect is again larger at higher temperatures. In the case of methylene groups, the role of the local water environment is less clear-cut: The increase of reorientational speed with the number of water molecules in the vicinity of a methylene group is less pronounced than that for amide groups; for $T \leq 350$ K, there is even a decrease in rotational speed at higher local water content. With the present data, it is not possible to determine unambiguously whether there exists a local antiplasticization effect due to hole filling, whether there is an indirect effect (water primarily alters the amide distribution and could, thus, change the chain structure around a methylene), or whether the observations are merely due to insufficient statistics.

Acknowledgment. We gratefully acknowledge financial support from the German Ministry of Education and Research (BMBF) through the Centre of Excellence in Materials Modelling and the Fonds der Chemischen Industrie. Computer time has been provided generously by the John-von-Neumann Institut für Computing at the Forschungszentrum Jülich. Authors are indebted to Pr. D. Brown for having provided the gmq software package.

References and Notes

(1) Reynaud, E.; Jouen, T.; Gauthier, C.; Vigier, G.; Varlet, J. *Polymer* **2001**, *42*, 8759.

(2) Miura, H.; Hirschinger, J.; English, A. D. *Macromolecules* **1990**, *23*, 2169.

(3) Loo, L. S.; Cohen, R. E.; Gleason, R. K. *Science* **2000**, *288*, 116.

(4) McCrum, N. G.; Read, B. E.; Williams, G. *Anelastic and dielectric effects in polymeric solids*; John Wiley: New York, 1967; p 484.

(5) Starkweather, H. W. Water in Nylon. *Water in Polymers*; ACS Symposium Series 127; American Chemical Society: Washington, DC, 1980; Chapter 25; p 433.

(6) Varlet, J.; Cavaille, J. Y.; Perez, J.; Johari, G. P. *J. Polym. Sci., Part B: Polym. Phys.* **1990**, *28*, 2691.

(7) Laredo, E.; Hernandez, M. C. *J. Polym. Sci., Part B: Polym. Phys.* **1997**, *35*, 2879.

(8) Pathmanathan, K.; Cavaillé, J. Y.; Johari, G. P. *J. Polym. Sci., Part B: Polym. Phys.* **1992**, *30*, 341.

(9) Neagu, R. M.; Neagu, E.; Kyritsis, A.; Pissis, P. *J. Phys. D: Appl. Phys.* **2000**, *33*, 1921.
(10) Garcia, J. M.; De La Campa, J. G.; De Abajo, J.; Ezquerra, T. A. *J. Polym. Sci., Part B: Polym. Phys.* **1997**, *35*, 457.
(11) Le Huy, H. M.; Rault, J. *Polymer* **1994**, *35*, 136.
(12) Laredo, E.; Grimau, M.; Sanchez, F.; Bello, A. *Macromolecules* **2003**, *36*, 9840−9850.
(13) Dlubek, G.; Redmann, F.; Krause-Rehberg, R. *J. Appl. Polym. Sci.* **2002**, *84*, 244.
(14) Rotter, G.; Ishida, H. *J. Polym. Sci., Part B: Polym. Phys.* **1992**, *30*, 489.
(15) Soldera, A.; Grohens, Y. *Macromolecules* **2002**, *35*, 722.
(16) Doxastakis, M.; Theodorou, D. N.; Fytas, G.; Kremer, K.; Faller, R.; Müller-Plathe, F.; Hadjichristidis, N. *J. Chem. Phys.* **2003**, *119*, 6883.
(17) Paul, W. In *Computational soft matter: from synthetic polymers to proteins, lecture notes*; Attig, N., Binder, K., Grubmueller, H., Kremer, K., Eds.; NIC Series; John Von Neumann Institute for Computing: Juelich, Germany, 2004; Vol. 23, p 169.
(18) Smith, G. D.; Borodin, O.; Paul, W. *J. Chem. Phys.* **2002**, *117*, 10350.
(19) Neyertz, S.; Brown, D.; Colombini, D.; Alberola, N. D.; Merle, G. *Macromolecules* **2000**, *33*, 1361.
(20) Roland, C. M.; Casalini, R. *Macromolecules* **2003**, *36*, 1361.
(21) Goudeau, S.; Müller-Plathe, F. *Macromolecules* **2004**, *37*, 8072−8081. Note that 24 really independent chains are generated in this work, whereas 3 independent chains were replicated using a scale-up procedure in order to obtain 24 chains in the reference work.
(22) Neyertz, S.; Brown, D. *J. Chem. Phys.* **2001**, *115*, 708.
(23) Brown, D. *gmq User Manual*, version 3; http://www.univ-savoie.fr/labos/lmops/brown/gmq.html; 1999.
(24) Brown, D.; Clarke, J. H. R.; Okuda, M.; Yamazaki, T. *J. Chem. Phys.* **1994**, *100*, 1684.
(25) Brown, D.; Clarke, J. H. R.; Okuda, M.; Yamazaki, T. *J. Chem. Phys.* **1994**, *100*, 6011.
(26) Brown, D.; Clarke, J. H. R.; Okuda, M.; Yamazaki, T. *J. Chem. Phys.* **1996**, *104*, 2078.
(27) Neyertz, S.; Brown, D.; Clarke, J. H. R. *J. Chem. Phys.* **1996**, *105*, 2076.
(28) Neyertz, S.; Brown, D. *J. Chem. Phys.* **1995**, *102*, 9725.
(29) For technical reasons, the PMC simulations of polyamide 6,6 with the gmq package required force field parameters slightly different from those presented in Table 1 of ref 21. A simplified model was used, with a charge of 0 on all atoms belonging to methylene moieties, −0.5 and +0.5*e* on the carbonyl oxygen and carbon, respectively, and −0.3 and +0.3*e* on the amide nitrogen and hydrogen, respectively. This provides electroneutrality in the treatment of the short-range nonbonded interactions.
(30) Viers, B. D. In *Polymer Data Handbook*; Mark, J. E., Ed.; Oxford University Press: New York, 1999; p 190.
(31) Berendsen, H. J. C.; Postma, J. P. M.; van Gunsteren, W. F.; DiNola, A.; Haak, J. R. *J. Chem. Phys.* **1984**, *81*, 3684.
(32) Müller-Plathe, F.; Brown, D. *Comput. Phys. Commun.* **1991**, *64*, 7.
(33) Müller-Plathe, F. *Comput. Phys. Commun.* **1993**, *78*, 77.
(34) Berendsen, H. J. C.; Grigera, J. R.; Straatsma, T. P. *J. Phys. Chem.* **1987**, *91*, 6269.
(35) Müller-Plathe, F.; van Gunsteren, W. F. *Polymer* **1997**, *38*, 2259.
(36) Brown, D.; Neyertz, S.; Douanne, A.; Bas, C.; Alberola, N. D. *J. Phys. Chem. B* **2002**, *106*, 4617.
(37) Müller-Plathe, F. *J. Chem. Phys.* **1998**, *108*, 8252.
(38) Rizzo, C. R.; Jorgensen, W. L. *J. Am. Chem. Soc.* **1999**, *121*, 4827−4836.
(39) Rizzo, C. R.; Jorgensen, W. L. *J. Am. Chem. Soc.* **2000**, *122*, 2878−2888.
(40) Kaminski, G. A.; Stern, H. A.; Berne, B. J.; Friesner, R. A. *J. Phys. Chem. A* **2004**, *108*, 621.
(41) Schaffer, M. A.; McAuley, K. B.; Cunningham, M. F. *Polym. Eng. Sci.* **2003**, *43*, 639.
(42) Rackaitis, M.; Strawhecker, K.; Manias, E. *J. Polym. Sci., Part B: Polym. Phys.* **2002**, *40*, 2339.
(43) A hydrogen-bond criterium is defined as follows: the distance between the hydrogen of the donor group and the acceptor has to be below 0.245 nm and the donor−hydrogen−acceptor angle above 130°. A water molecule can share (as the donor) two hydrogen bonds with the amide carbonyl group and one bond (as the acceptor) with the amide NH group.
(44) Müller-Plathe, F. *Macromolecules* **1998**, *31*, 6721.
(45) Kotelyanskii, M. J.; Wagner, N. J.; Paulaitis, M. E. *Comput. Theor. Polym. Sci.* **1999**, *9*, 301.
(46) The lower activation energies, E_γ, and relaxation times obtained with PA10 are not in contradiction with the apparent stiffening effect of water at low temperatures and time scales. Slightly different KWW exponents in pure and water-containing systems allow a crossover of $OACF_{(PA10)}$ and $OACF_{(PA0)}$ between the short-time regime (t < 100 ps, $OACF_{(PA10)} > OACF_{(PA0)}$) and the long-time one ($t \gg 1$ ns, $OACF_{(PA10)} < OACF_{(PA0)}$).
(47) Starkweather, H. W.; Barkley, J. R. *J. Polym Sci., Part B: Polym. Phys.* **1981**, *19*, 1211.